Automatic Selection of the WPT Decomposition Level for Condition Monitoring of Rotor Elements Based on the Sensitivity Analysis of the Wavelet Energy

Cristina Castejón, María Jesús Gómez, Juan Carlos García-Prada, Alberto Junior Ordoñez and Higinio Rubio

MAQLAB Group, Mechanical Dept. Universidad Carlos III de Madrid, Av. de la Universidad, 30, 28911, Madrid, Spain

(Received 25 January 2013; accepted 24 February 2014)

Vibration signals are a widely used technique for machine monitoring and fault diagnostics. However, it is necessary to select a suitable pattern that represents the condition of the machine. Wavelet Packet Transform (WPT) provides a high potential for pattern extraction. Several factors must be selected and taken into account in the wavelet transform application such as the level of decomposition, the suitable mother wavelet, and which frequency bands (obtained from the decomposition process) contain the necessary information for the diagnosis system. The selection of the parameters commented above is a complex task that depends on many factors. Most of the works found in the literature select these factors based on experience, graphical methods, or trial and error methods. In this work, a method based on the relative wavelet energy is developed in order to automatically select the parameter defined by the WPT. The selection allows for the efficient extraction of the most suitable patterns for a later classification and fault detection process. In order to prove the soundness of the method proposed, a Jeffcott rotor model with four crack levels will be developed, and the vibratory signals provided by this model will be used for the monitoring condition.

NOMENCLATURE

WT	Wavelet Transform
FT	Fourier Transform
MRA	Multirresolution Analysis
ANN	Artificial Neural Network
CWT	Continuous Wavelet Transform
DWT	Discrete Wavelet Transform
WPT	Wavelet Packets Transform
Db6	Daubechies 6
RBF	Radial Basis Function Neural Network

1. INTRODUCTION

The study of the vibration signal is a main technique in the study and diagnosis of the failures in rotator and structural elements, which is one of the main objectives in condition-based maintenance. The concepts, procedures, and challenges of this kind of maintenance are consolidating for real industrial practice.[1] There are several methods focused in the fault detection, mainly with the intention of extracting behaviour patterns able to identify a failure. Among them, the Wavelet Transform (WT) is one of the techniques that has been adopted by a vast amount of applications, frequently replacing the conventional Fourier Transform (FT); however, sometimes it is still used in combination with other techniques as intelligent classifiers, as in the case of Wang and Chen.[2] Peng et al. carried out a bibliographical review on the application of WT on vibration signals to monitoring and fault diagnosis in machines.[3] Researchers such as Douka et al. have developed a method of crack identification for structures based on the continuous wavelet analysis.[4] Adewusi[5] presented an experimental study, using the wavelet analysis in vibratory signals provided by a rotor. In this previous work, the configuration was performed in a cantilever and with a V-notch of 4 mm, propagating a transversal crack.

Specifically for industrial maintenance, the diagnostics of cracked rotors is a critical subject. This area has focused the attention of many researchers in the last decades. A lot of studies about the dynamics of cracked rotating machinery have been carried out with different methods in order to detect the effects of cracks. Concretely, dynamics and modelling of cracked shafts have been highly developed; however, the inverse problem of the identification of cracks has not been commonly included.[6] A lot of studies have tried to characterize the behaviour of rotors.[7,8] Some wide reviews about the behaviour and modelling of cracked rotating machinery can be consulted,[9,10] as well as more recent studies about this issue.[11] The most common cracks are superficial and transversal that breathe, i.e, that open and close during rotation. There are a lot of theoretical works that propose models of the breathing phenomena.[6] Some classical approximations are the Gash function[12] and the Mayes and Davies function.[13] A review of the classical and modern breathing functions can also be consulted.[14]

Related to rotatory elements, WT theory combined with intelligent classification systems has been applied with success in the last decade in vibration signals from rotors[15] rolling bearing elements using the Continuous Wavelet Transform (CWT)[16] or Discrete Wavelet Transform (DWT).[17,18] In all cases, the selection of the mother wavelet for the transformation is carried out based on experience, and the test of the

most common mother wavelet is used (Morlet, Haar, and the Daubechies family). Related to the level of decomposition, the process is the same, and the authors represent and test different decomposition levels and select the level that presents the biggest differences between the conditions. With non-stationary signals, that means that we are not sure if the selection is the optimum for our purpose, and, obviously, if the machine condition changes (load, rolling element type, or geometry) the patterns will not be the most representative.

Wavelet Packet Analysis (WPT) is based in the DWT analysis, and consists of an improvement of the MRA. Wavelet Packets coefficients can be directly used as features, and they present a high sensibility to failures.[19] In summary, many kinds of fault characteristics can be obtained, principally with the Wavelet coefficients or the Wavelet energy. Since the Wavelet coefficients will highlight the changes in signals, which often predict the occurrence of the fault, the Wavelet coefficients-based features are suitable for early fault detection. However, because slight changes on signals often have small energy, these changes will be easily masked in Wavelet energy-based features.

In the present work, the energy of the coefficients obtained from the WPT will be used in order to automatically select the feature pattern that better describes the fault condition. The mother wavelet applied will be the Daubechies 6 (db6). The coefficients obtained will be used to calculate the energy values in many frequency bands, which will help to find failure patterns to make reliable diagnoses. The study also shows a novel methodology to select the most suitable decomposition level for all applications. The methodology allows the automatic selection of this level. The method will be applied to vibratory signals obtained from the startup of a Jeffcott rotor model that includes the Gash breathing function to model the cracks.

2. WAVELET PACKETS TRANSFORM

Wavelet packets transform (WPT) is a generalized form of the Discrete Wavelet Transform (DWT). The DWT of a signal $\mathbf{x} = \{x[i]\}$ is decomposed simultaneously using a high-pass filter (h) and a low pass filter (g) with impulse response. Output gives the detail coefficients (D) from the high-pass filter and the approximation coefficients (A) from the low-pass one.[20] It is important to note that both filters are related one to each other, and they are known as a quadrature mirror filter. However, since half of the frequencies of the signals have now been removed, half of the samples can be discarded according to Nyquist's rule.[21] The filter outputs are then downsampled by two as Eq. (1):

$$y_{\text{low}}[n] = \sum_{i=0}^{N} x[i]\, g[2n - i];$$
$$y_{\text{high}}[n] = \sum_{i=0}^{N} x[i]\, h[2n - i]; \qquad (1)$$

where N is the size of the signal $\mathbf{x}$. This decomposition has halved the time resolution since only half of each filter output characterizes the signal. However, each output has half the frequency band of the input so the frequency resolution has been doubled.

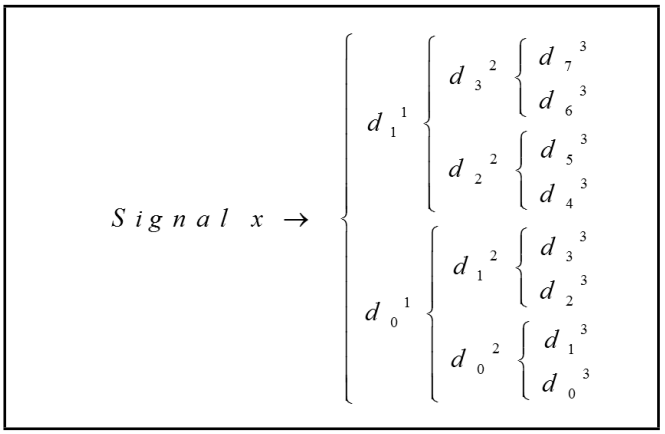

Figure 1. WPT coefficients nomenclature for a decomposition level of 3.

The downsampled signals from the low-pass filter and high-pass filter are referred to as first-level approximation (A) and detail (D) coefficients, respectively. To get the second-level, the application of the filters to coefficients A and D gives as result the approximation of approximation (AA), detail of approximation (DA), approximation of detail (AD), and detail of detail (DD) coefficients, the same procedure is repeated for the rest of levels.

The number of packets generated corresponds to 2^k where k is the decomposition level. As an example, for a decomposition level 3, 8 packets are obtained and for a level 10, 1024 packets will be generated. At every level of decomposition, the frequency resolution is doubled when filtered while the time resolution is halved by downsampling operation. This decomposition is repeated to further increase the frequency resolution and to reduce the amount of approximation coefficients. This is represented as a binary tree with nodes in a sub-space with different time-frequency localization, and it is shown in Fig. 1.

The tree presented is known as a filter bank.[17] At each level, the signal is decomposed into low and high frequencies. For example, using a sample frequency of 5000 Hz, the bandwidth that can be reconstructed is 2500 Hz. In this case, the bandwidth covered by each packet for decomposition level 3 corresponds to 312.5 Hz, while the range of each packet for a decomposition level 10 is 2.4 Hz, which corresponds to a quite narrow band. The reduction of bandwidth as the WPT decomposition level increases can be seen in Fig. 5a. Due to the decomposition process, the input signal must be a multiple of 2^k.

2.1. Relative Wavelet Energy

The energy concept used in the WPT analysis is related to the known concept derived from the Fourier theory.[19] As a previous step to the energy calculus, the selection of a mother wavelet $\psi(t)$ and the decomposition level k must be done. The energy (E_j) of each packet (j) at each decomposition level (k), is obtained from the energy of the coefficients of each packet that can be represented as $\mathbf{d_j^k} = \{d_j^k(1), d_j^k(2), \ldots, d_j^k(n)\}$, where n is the number of coefficients of each packet j. Then, the energy of each packet is calculated as shown in Eq. (2):

$$E_j = \sum_{i=1}^{n} \left| d_j^k(i) \right|^2. \qquad (2)$$

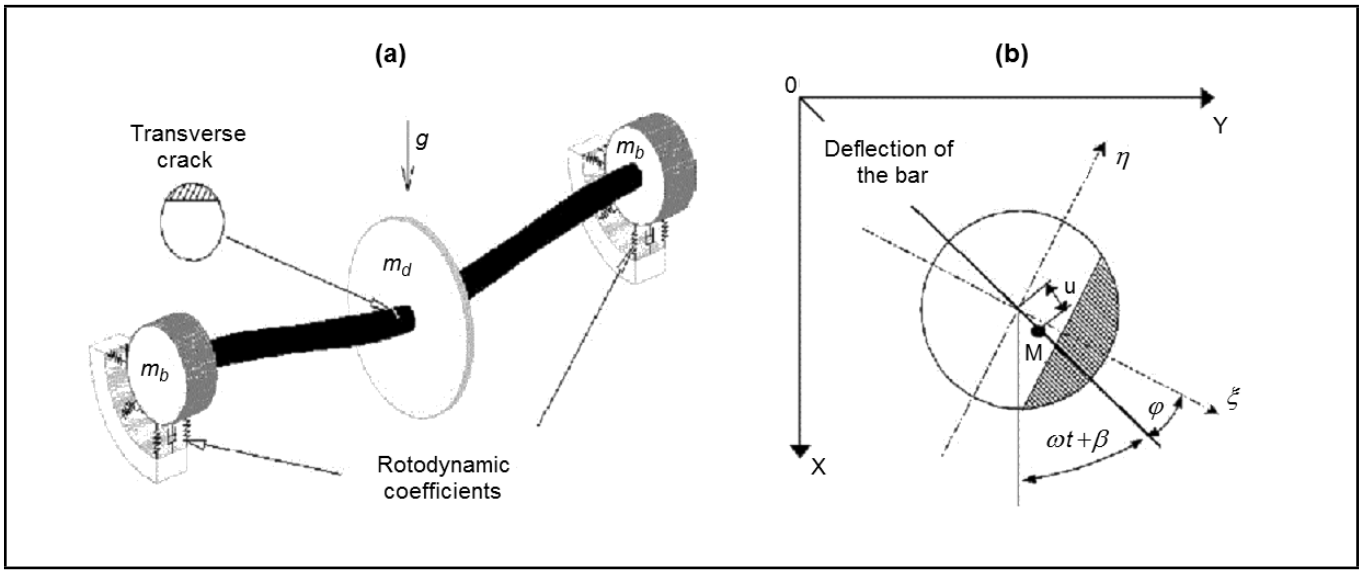

Figure 2. (a) Schematic of rotor system with a crack at shaft mid-span indicating disc mass imbalance and crack relative orientations. (b) Coordinate system.

Table 1. Jeffcott model parameters.

Case	Shaft Diameter	Shaft Length	Disc Ratio	Disc Mass	Imbalance Mass	Nat. Freq. Flex	β	ΔK_1	ΔK_1 (Range)
1	0.0157 m	0.3225 m	0.05 m	1.8 kg	2.10^{-4}	48 Hz	0°	0.0	[0.00:0.001:0.011]
2							90°	0.05	[0.038:0.002:0.060]
3							180°	0.12	[0.108:0.002:0.13]
4							270°	0.22	[0.206:0.002:0.228]

In order to obtain the relative energy, the whole signal energy must be calculated before decomposition by means of Eq. (3):

$$\mathbf{E} = \sum_{i=1}^{N} E_j; \tag{3}$$

where N is the number of packets and is $N = 2^k$. Finally, relative energy is defined by Eq. (4):

$$\rho_j = \frac{E_j}{\mathbf{E}}, \qquad j = 0, \ldots, N-1; \tag{4}$$

where:

$$\sum_j \rho_j = 1. \tag{5}$$

3. TEST VIBRATORY SIGNALS

With the aim of obtaining a set of signals to validate the method proposed, a modified Jeffcott rotor has been modelled.[8,22] The model has been developed with the software MATLAB™ and Simulink™. The model includes a crack localized in the midspan related to the supports.

In Fig. 2a the Jeffcott rotor can be seen. The crack is oriented in the transversal direction. In Fig. 2b, a transversal section of the crack and the axle is presented. In this figure besides the coordinate system selected an unbalance M can be positioned in the 2π rad of the disc. The fault conditions defined are the following: shaft without crack 0%, slight crack of 12.5% related to the axle diameter, medium crack 25%, and severe crack corresponding to 50%. The stiffness variation is represented in Eq. (6):

$$\Delta K_1 = \frac{\Delta K\xi + \Delta K_\eta}{K_s}; \tag{6}$$

where $\Delta K\xi$ and ΔK_η are the variation of the stiffness in ξ and η directions respectively. K_s is the full axle stiffness. So, $\Delta K_1 = 0$ corresponds to an axle without a crack, $\Delta K_1 = 0.05$ to a slight crack, $\Delta K_1 = 0.12$ to a medium crack, and $\Delta K_1 = 0.22$ to a severe crack. In order to obtain a complete set of signals with the four subset conditions, two parameters will be modified in the model: the crack depth (ΔK_1) and the unbalance orientation related to the crack (β angulus in Fig. 2b). In Table 1, the summary of all the simulations carried out is presented. The range of the crack depth has been modified in increments of 0.002 and several simulations with four different unbalance orientations have been done.

The four subsets generated are combined with the four unbalance orientations, which are $\beta = 0$; $\beta = \pi/2$; $\beta = \pi$; $\beta = 3\pi/2$. A total of 195 signals have been obtained from the different models.

In Fig. 3 the response in y direction of the four conditions studied in the start-up state (transitory state) are presented versus the speed ratio with respect to the final velocity to reach. In all cases, the final velocity is 2.2 times the critical speed of the system, and the sample frequency used is 5000 Hz (bandwidth 2500 Hz).

4. RELATIVE WAVELET ENERGY ANALYSIS

After discussing the theoretical bases and obtaining a set of signatures needed for the test and validation, the process presented in this paper is developed. Vibratory signal corresponds to the first 10 seconds of the actuator start up (transitory state). The signal is decomposed by means of WPT using decomposition levels from 3 to 10. At this stage, packets capacity to contain information to detect and classify defects at any level k of the WPT is not dismissed. For each packet generated, relative wavelet energy is calculated. At a descendent sort, feature

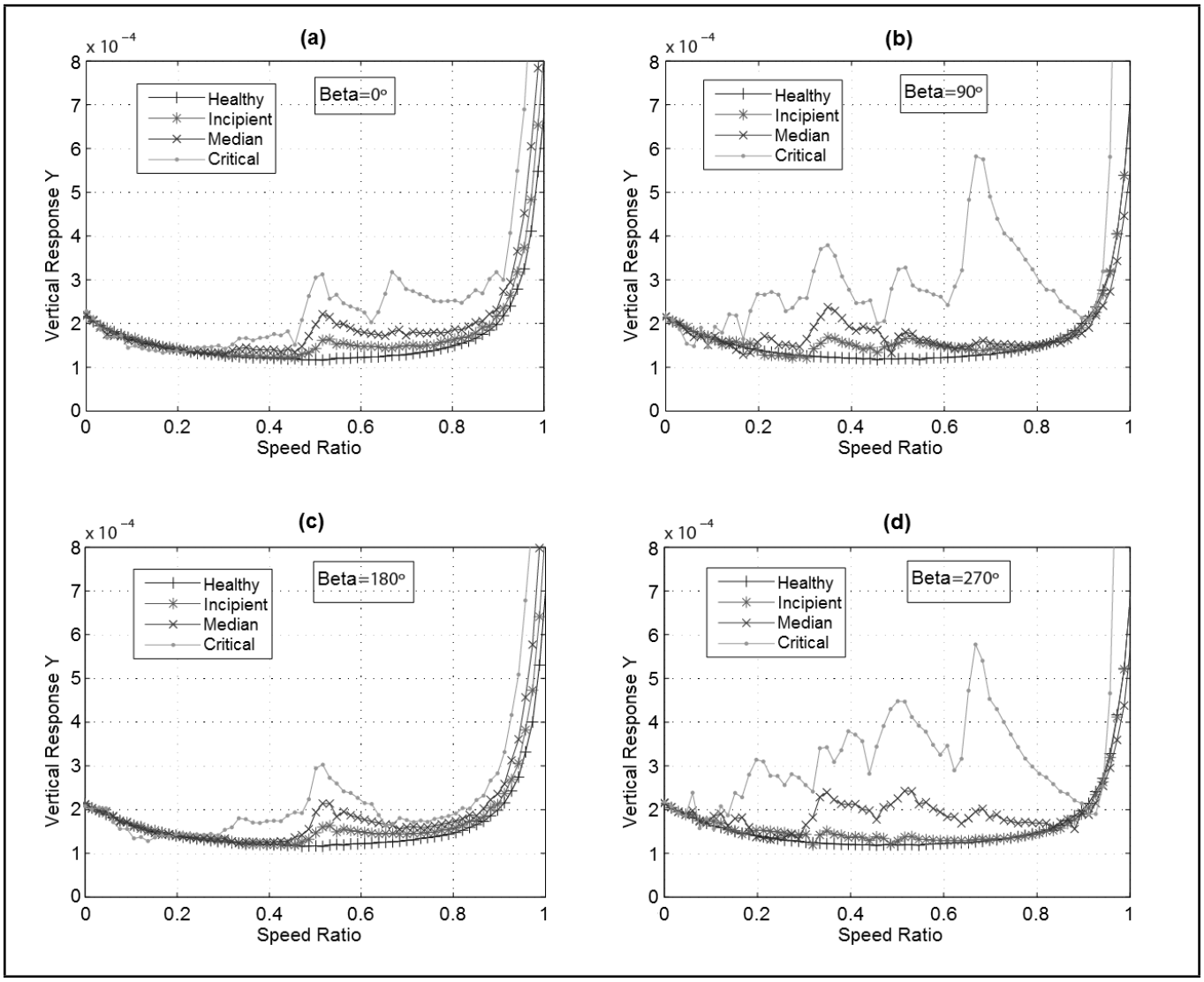

Figure 3. Vibratory signatures from the Jeffcott rotor model for different β values and for each shaft condition. Case (a) corresponding to an unbalance orientation respect to the crack of 0 rad, (b) corresponding to an unbalace of $\pi/2$ rad, (c) and (d) for an unbalance of π and $3\pi/2$ rad, respectively. Notice that the unbalance orientation of cases (b) and (d) present higher amplitudes.

vectors are generated by the wavelet coefficients included in the first four packets with greater increments in energy. The greater increments in energy are calculated as the bigger differences between the energy of the signals of all the crack conditions studied regarding the case of healthy shaft. These increments of energy when a crack appears are called Δe.

Table 2 shows the procedure for a WPT decomposition level range from 3 to 10, where characteristic patterns are obtained, and ordered by importance. The first column represents the levels of decomposition, the column labeled "First..." which is divided into two columns, corresponds to the packet with the higher relative energy with his frequency band in Hz. At WPT level 3, the biggest changes in the relative energy occur in the package of approximation coefficients or the also called zero level (0). This is because the band has the highest concentration of the most important information, which is at low frequencies, while high frequencies are the details or nuances of the signal. For example, in the case of the human voice, if high frequency components are removed, the voice sounds different, but its message is understood. However, if low frequency components are deleted, the message becomes unrecognizable. In this work, the nuances are due to the presence of cracks, and in the transformation they are transferred to the high frequency or levels of detail. The level of detail most affected by the presence of the crack will therefore absorb this energy, which indicates the presence of a defect or phenomenon to mention in general. After zero level the following packages with the higher relative energy are 1, 3, and 6 (in the case of WPT level 3). The decomposition continues until level 10 is reached. For the signals used and processed by this method, the levels with higher relative energy changes are 8, 9, and 10.

As can be observed, discarding the zero level in high decomposition levels where the bandwidth is narrower, it can be affirmed that the bigger increments in energy when a crack appears are always in the packet that holds the natural frequency of 48 Hz. The cell that contains the natural frequency at each decomposition level is shaded in all cases in Table 2.

Based on the results, an ANN is used in order to make a smart sort and validate both the performance and efficiency for each decomposition level. In this work a Radial Basis Neural Network (RBF) has been designed[23] to measure the potential of the selected patterns. The training has been conducted with a distribution of input patterns (obtained from the Jeffcott rotor model) corresponding to 75% for training and 25%

Table 2. Coefficient number and bandwidth for the four packets with the higher Δe regarding the healthy condition for different decomposition levels.

	First Δe packet		Second Δe packet		Third Δe packet		Fourth Δe packet	
WPT level	1st	WideBand [Hz]	2nd	WideBand [Hz]	3rd	WideBand [Hz]	4th	WideBand [Hz]
3	d_0^3	0–312.5	d_1^3	312.5–625	d_3^3	625–937.5	d_6^3	1250–1562
4	d_0^4	0–156.3	d_1^4	156.3–312.5	d_3^4	312.5–468.8	d_2^4	468.8–625
5	d_0^5	0–78.1	d_1^5	78.1–156.3	d_3^5	156.3–234.4	d_7^5	390.6–468.8
6	d_0^6	0–39.1	d_1^6	39.1–78.1	d_3^6	78.1–117.2	d_2^6	117.2–156.3
7	d_0^7	0–19.5	d_3^7	39.1–58.6	d_1^7	19.5–39.1	d_7^7	97.7–117.2
8	d_0^8	0–9.8	d_6^8	39.1–48.8	d_2^8	29.3–39.1	d_7^8	48.8–58.6
9	d_0^9	0–4.9	d_{13}^9	43.9–48.8	d_{12}^9	39.1–43.9	d_5^9	29.3–34.2
10	d_0^{10}	0.00–2.4	d_{26}^{10}	46.4–48.8	d_{27}^{10}	43.9–46.4	d_{10}^{10}	29.3–31.7

for testing. In Fig. 4, the process of optimization of the RBF neural network can be observed. The network is trained with 22 neurons in the hidden layer and a spread value of 1. The percentage of efficiency is determined for the first three bands with higher Δe, deleting the first one or approximation band, which contains information of energy that lately can be transferred to higher levels. Figure 4a shows the bandwidth for each level of decomposition of the range selected. As can be seen, when the decomposition level increases, the band is reduced (narrowed), refining the area with the highest energy change. In Fig. 4b the success rates of classification depending on the decomposition level are presented. The classification for level $N = 3$ achieved about a 25% success rate for the three optimal bands. There is an improvement in the levels $N = 4, 5, 6$. For the level $N = 7$ the results are about 97% for the first band and are 100% for the second and third. After that, for levels 8, 9, and 10, a success rate of 100% is achieved also for the first and third band, and 97% for the second one.

The bandwidth is more different with respect to the healthy rotor, in terms of energy, and is 46.4–48.8 Hz. This range covers very precisely the natural frequency of the system, which is 48 Hz. It can be concluded that the presence of a crack significantly affects the energy nearby the natural frequencies.

As the decomposition level decreases, less information is available to detect failure patterns, but also the computational cost is reduced. For this reason, the optimal decomposition level to achieve is the lowest possible that gives a success rate in the classification higher than a limit imposed and that allows locating the failure in a narrow enough bandwidth. For example, in this case, if the limit of classification is set to 98%, and a bandwidth of less than 10 Hz is imposed, the optimal decomposition level is 8.

5. CONCLUSIONS AND FUTURE WORK

In this paper, the extraction and automatic selection of patterns through the application of the WPT and analysis of the relative energy of wavelet packets for either incipient fault level or higher has been presented. The method lets selecting the approximation and detail level that can discretize the problem by creating defects codes that are easily adaptable to automatic diagnosis and classification.

This demonstrates that the WPT technique is an excellent tool for the extraction of characteristic patterns of vibration signals, even in the incipient fault diagnosis. Concretely, the energy of WPT has proven its reliability, because the frequency band that holds bigger differences with the healthy rotor corresponds to the natural frequency, as could be predicted.

Intelligent classification systems are used to optimize the process of analysis and selection of patterns, making comparisons with high sensitivity levels. The best patterns extracted from vibration signals are processed by WPT and classified efficiently using RNA levels of accuracy above 97%.

As future work, the authors think that it would be very interesting to prove the reliability of this method in experimental signals obtained from real systems in order to improve the predictive maintenance of turbomachinery. Also it would be very useful to prove the effectiveness of this methodology in systems that do not reach high speeds.

ACKNOWLEDGEMENTS

The financial support of the regional government of Madrid and Carlos III University is gratefully acknowledged through the Project MADBOT 2011/00130/001.

REFERENCES

[1] Ahmad, R., Kamaruddin, S. An overview of time-based and condition-based maintenance in industrial application, *Computers & Industrial Engineering*, **63**, 135–149, (2012).

[2] Wang, H., Chen, P. Intelligent diagnosis method for rolling element bearing faults using possibility theory and neural network, *Computers & Industrial Engineering*, **60**, 511–518, (2011).

[3] Peng, Z., Chu, F. Application of the wavelet transform in machine condition monitoring and fault diagnostics: a review with bibliography, *Mechanical Systems and Signal Processing*, **18**, 199–221, (2004).

[4] Douka, E., Loutridis, S., Trochidis, A., Crack identification in beams using wavelet analysis, *International Journal of Solids and Structures*, **40**, 3557–3569, (2003).

[5] Adewusi, S. A. Wavelet analysis of vibration signals of an overhang rotor with a propagating transverse crack, *Journal of Sound and Vibration*, **5**, 777–793, (2001).

[6] Bachshmid, N., Penacci, P., Editorial, Crack effects in rotordynamics, *Mechanical Systems and Signal Processing*, **22**, 761–762, (2008).

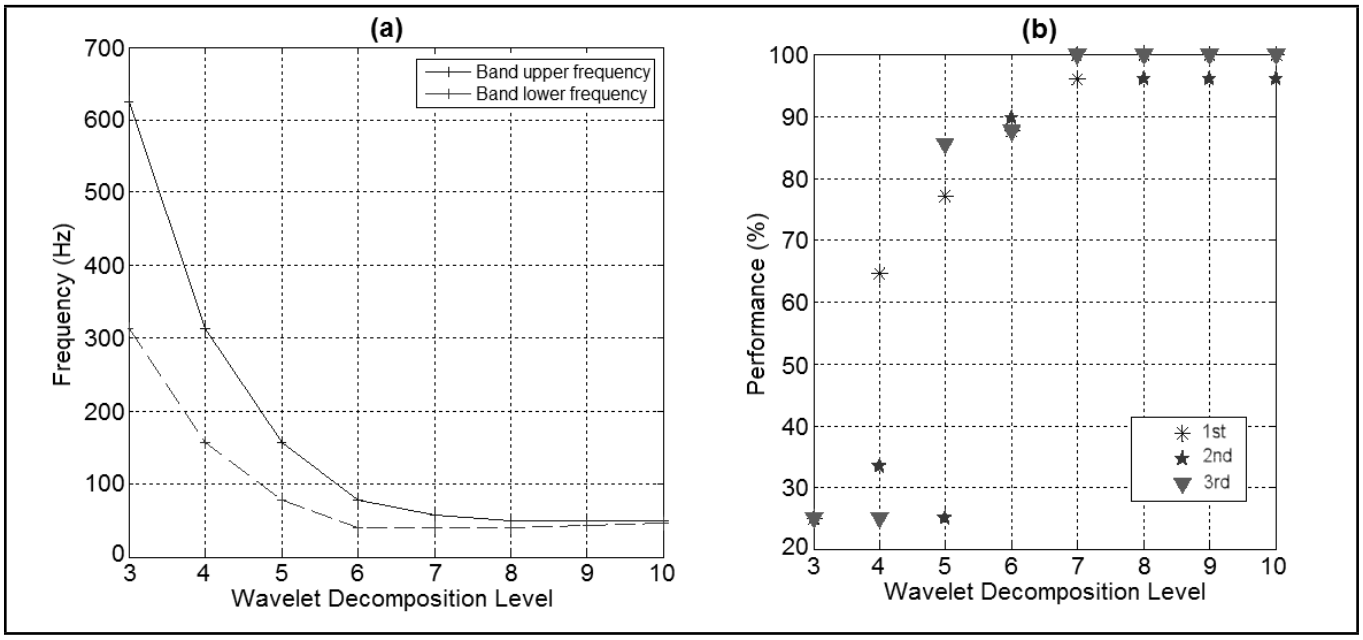

Figure 4. Optimum frequency band and classification performance.

[7] Chancey, V. C., Flowers, G. T., Howard, C. L. Characterisation of transient behaviours in rotordynamic vibrations from experimental data using harmonic wavelets, *International Journal of Acoustics and Vibration*, **6**, 15–22, (2001).

[8] Diken, H., Alnefaie, K. Startup dynamic behaviour of a Jeffcott rotor, *International Journal of Acoustics and Vibration*, **10**, 83–88, (2005).

[9] Gasch, R. Dynamic behavior of the Laval rotor with a transverse crack, *Mechanical Systems and Signal Processing*, **22**, 790–804, (2008).

[10] Bachschmid, N., Penacci, P., Tanzi, E. Some remarks on breathing mechanism on non-linear effects and on slant and helicoidal cracks, *Mechanical Systems and Signal Processing*, **22**, 879–904, (2012).

[11] Kulesza, Z., Sawicki, J. T. Rigid finite elements model of a cracked rotor, *Journal of Sound and Vibration*, **331**, 4145–4169, (2012).

[12] Gash, R. Dynamic behavior of a simple rotor with a cross-sectional crack, *Proc. Institution of Mechanical Engineers Conference on Vibration in Rotating Machinery*, 178/76, Cambridge, UK, (1976).

[13] Mayes, I. W. and Davies, W. G. R. The vibrational behavior of a rotating shaft system containing a transverse crack, *Proc. Institution of Mechanical Engineers Conference on Vibration in Rotating Machinery*, 168/76, Cambridge, UK, (1976).

[14] Al-Schudeifat, M. A. and Butcher, E. A. New breathing functions for the transverse breathing crack of the cracked rotor system: Approach for critical and subcritical harmonic analysis, *Journal of Sound and Vibration*, **330**, 526–544, (2011).

[15] Srinivas, H. K., Srinivasan, K. S., Umesh, K. N. Role of an artificial neural network and a wavelet transform for condition monitoring of the combined faults of unbalance and cracked rotors, *International Journal of Acoustics and Vibration*, **15** (3), 121–127, (2010).

[16] Li, L., Qu, L., Liao, X. Haar wavelet for machine fault diagnosis, *Mechanical Systems and Signal Processing*, **21**, 1773–1786, (2007).

[17] Castejón, C., Lara, O., Garcia-Prada, J. Automated diagnosis of rolling bearings using MRA and neural networks, *Mechanical Systems and Signal Processing*, **24**, 289–299, (2010).

[18] Lei, Y., He, Z., Zi, Y. Application of an intelligent classification method to mechanical fault diagnosis, *Expert Systems with Applications*, **36** (6), 9941–9948, (2009).

[19] Hu, Q., He, Z., Zhang, Z., Zi, Y. Fault diagnosis of rotating machinery based on improved wavelet package transform and svms ensemble, *Mechanical system and signal processing*, **21**, 688–705, (2007).

[20] Mallat, S. *A Wavelet Tour of Signal Processing*, Academic Press, (1998).

[21] Polikar, R. *The Wavelet Tutorial*, Rowan University, College of Engineering, (1996).

[22] Litak, G., Sawicki, J. T. Intermittent behaviour of a cracked rotor in the resonance region, *Chaos, Solitons & Fractals*, **42** (3), 1495–1501, (2009).

[23] Lara, O., Castejón, C., Garcia-Prada, J. Bearing fault diagnosis based on neural network classification and wavelet transform, *WSEAS Transaction on Signal Processing*, **2** (10), 1371–1378, (2006).